AIMS Mathematics, 9(7): 18506–18527.
DOI:10.3934/math.2024901
Received: 05 April 2024
Revised: 03 May 2024
Accepted: 13 May 2024
Published: 03 June 2024

http://www.aimspress.com/journal/Math

Research article

Research on pattern dynamics of a class of predator-prey model with interval biological coefficients for capture

Xiao-Long Gao[1], **Hao-Lu Zhang**[2,4] **and Xiao-Yu Li**[3,*]

[1] Department of Mathematics, Inner Mongolia University of Technology, Hohhot 010051, China
[2] CCCC Comprehensive planning and Design Institute Co., Ltd, Beijing 100024, China
[3] College of Date Science and Application, Inner Mongolia University of Technology, Hohhot 010080, China
[4] School of Civil Engineering, Inner Mongolia University of Technology, Hohhot 010051, China

* **Correspondence:** Email: fish-li82@163.com; Tel: +864716575470; Fax: +864716575863.

Abstract: Due to factors such as climate change, natural disasters, and deforestation, most measurement processes and initial data may have errors. Therefore, models with imprecise parameters are more realistic. This paper constructed a new predator-prey model with an interval biological coefficient by using the interval number as the model parameter. First, the stability of the solution of the fractional order model without a diffusion term and the Hopf bifurcation of the fractional order α were analyzed theoretically. Then, taking the diffusion coefficient of prey as the key parameter, the Turing stability at the equilibrium point was discussed. The amplitude equation near the threshold of the Turing instability was given by using the weak nonlinear analysis method, and different mode selections were classified by using the amplitude equation. Finally, we numerically proved that the dispersal rate of the prey population suppressed the spatiotemporal chaos of the model.

Keywords: interval biological coefficient; fractional predator-prey model; weakly nonlinear analysis; Hopf bifurcation
Mathematics Subject Classification: 65L10, 65R20

1. Introduction

With the development of human civilization, maintaining ecological balance has become a major challenge facing mankind. The predator-prey model is a mathematical model for studying the interaction between predators and prey in ecosystems [1, 2]. It can be used to analyze the impact of environmental changes or the introduction of new species. At present, about 28% of the assessed species in the world are at risk of extinction [3]. In response to this situation, the implementation of

a reasonable policy for the development of biological resources can protect populations from possible extinction [4].

Yan [5] studied the global stability of a delayed diffusion predator-prey model with Michaelis-Menten-type prey capture. Ou [6] obtained the parameter conditions for the stability and bifurcation of two delayed predator-prey systems. Yao [7] studied the dynamics of a Leslie-Gower predator-prey system with proportionally dependent Holling IV functional response and a constant prey capture rate. Zhang [8] applied a delayed predator-prey model with non-constant mortality and a constant prey capture rate to investigate the effect of time delay on equilibrium stability. Chen [9] studied the pattern dynamics of a harvested predator-prey model with no-flux boundary conditions. Cui [10] proposed a new Lotka-Volterra commensal symbiosis system accompanying delay. Therefore, motivated by the above discussion, we consider the following predator-prey model with a harvesting term:

$$\begin{cases} \frac{\partial u}{\partial t} = d_1 \Delta u + u(1-u) - \frac{auv}{u+v} - bu, \\ \frac{\partial v}{\partial t} = d_2 \Delta v + \frac{\beta uv}{u+v} - \alpha v, \end{cases} \tag{1.1}$$

where $u(x,t)$ and $v(x,t)$ represent the densities of the prey and predators at location x and time t, respectively. Δ is the Laplacian operator. d_1 and d_2 represent the diffusion rates of prey u and predator v, respectively. a and β are two positive constants. bu implies harvesting of the prey population, and αv denotes harvesting of the predator population.

It can be seen from the existing literature that the parameters in most biological models are considered to be accurate. However, due to factors such as climate change, natural disasters, and deforestation, most measurement processes and initial data may have errors [11]. Therefore, models with imprecise parameters are more realistic. A model with imprecise biological parameters can be reflected by random, fuzzy, and interval methods. In fuzzy methods, imprecise parameters are represented in the form of fuzzy sets or fuzzy numbers. Nowadays there are many studies on fuzzy parameters of dynamical systems [12, 13]. In the stochastic method, imprecise parameters are represented by random variables with appropriate probability distribution [14, 15]. Different from random and fuzzy methods, Pal [16] first proposed the concept of an interval to describe the imprecise parameters of ecological models. This method is easier and more effective than the first two methods. Since then, many scholars have used an interval method to study ecological models with inaccurate parameters. Pal uses the exponential form of interval parameters, and Ramezanadeh uses the linear form of interval parameters [17, 18].

Fractional derivatives have memory and nonlocality. In biological systems, memory refers to the ability of the system to retain the information of past events and use it to influence future behavior [19–22]. Due to the fact that most populations have long-term memory [23, 24], integer order population systems ignore the influence of memory. Therefore, we consider a fractional order predator-prey model. There are many ways to solve fractional differential equations, for example, the fractional reduced differential transform method [25], the Adomian decomposition sumudu transform method [26], the Fourier spectral method [27–30], and the piecewise reproducing kernel method [31]. In this paper, the Euler discrete method is used. It can describe the ecological process of the reaction-diffusion equation on a long time scale and has the advantage of fast calculation speed.

The main contributions of this paper are as follows:

1) Due to other factors, most measurement processes and initial data may have errors. In this paper, a more realistic interval parameter model is used.

2) The Turing pattern is theoretically classified and verified by numerical methods. Some different results are obtained.
3) We numerically prove that the dispersal rate of the prey population will suppress the spatiotemporal chaos of the model.

The rest of this article is organized as follows: In Section 2, we establish a model and explore the positivity and uniqueness of solutions for models without diffusion terms. In Section 3, we discuss the stability of the model and Hopf bifurcation. In Section 4, the Turing instability of the model is discussed. In Section 5, weak nonlinear analysis is used to derive the amplitude equation. In Section 6, we conduct numerical simulations. Conclusions are given in Section 7.

2. Model and preliminaries

2.1. Model formation

To establish our model, we introduce the following two definitions.

Definition 2.1. *([16, 18, 32]) An interval number A is defined by* $A = [\acute{a}, \grave{a}] = \{y|\acute{a} \leq y \leq \grave{a}, y \in \mathbb{R}\}$. *Moreover, each real number* $a \in \mathbb{R}$ *can be represented by* $[a, a]$. *Let* $A = [\acute{a}, \grave{a}]$ *and* $B = [\acute{a}, \grave{a}]$. *Define the following algorithms:*

1) $A + B = [\acute{a}, \grave{a}] + [\acute{b}, \grave{b}] = [\acute{a} + \acute{b}, \grave{a} + \grave{b}]$ for $\acute{a} + \acute{b} > 0$;
2) $A - B = [\acute{a}, \grave{a}] - [\acute{b}, \grave{b}] = [\acute{a} - \acute{b}, \grave{a} - \grave{b}]$ for $\acute{a} - \acute{b} > 0$;
3) $\rho A = \rho\,[\acute{a}, \grave{a}] = [\rho\acute{a}, \rho\grave{a}]$ for $\rho \geq 0$;
4) $\rho A = \rho\,[\acute{a}, \grave{a}] = [\rho\grave{a}, \rho\acute{a}]$ for $\rho < 0$.

Definition 2.2. *([16, 18, 32]) Let* $a > 0$ *and* $b > 0$ *have interval* $[a, b]$. *The interval-valued function is presented as* $f(r) = a^{1-r}b^r$ *for* $r \in [0, 1]$.

Some authors have found that the dynamic behavior of a fractional model [33–36] is much more complex than that of the corresponding integer model. According to Definition 2.1, we consider the following fractional predator-prey model with interval biological coefficient

$$\begin{cases} D_t^{\alpha} u = d_1 \Delta u + u(1-u) - \frac{[\acute{a}, \grave{a}]uv}{u+v} - [\acute{b}, \grave{b}]u, \\ D_t^{\alpha} v = d_2 \Delta v + \frac{[\acute{\beta}, \grave{\beta}]uv}{u+v} - [\acute{\alpha}, \grave{\alpha}]\, v, \end{cases} \tag{2.1}$$

where $\acute{a} > 0, \acute{b} > 0, \acute{\alpha} > 0$, and $\acute{\beta} > 0$. Now, there are many types of fractional derivatives [34–38]. Here, D_t^{α} represents Caputo fractional differentiation. It has the advantage of relatively simple calculation, which is defined as follows:

$$D_t^{\alpha} u(t) = \frac{1}{\Gamma(1-\alpha)} \int_0^t (t-\tau)\, u'(\tau)\, \mathrm{d}\tau \ , t > 0. \tag{2.2}$$

Using Definition 2.2, we get

$$\begin{cases} D_t^{\alpha} u = d_1 \Delta u + u(1-u) - \frac{\grave{a}^{1-r}\acute{a}^r uv}{u+v} - \grave{b}^{1-r}\acute{b}^r u, \\ D_t^{\alpha} v = d_2 \Delta v + \frac{\acute{\beta}^{1-r}\grave{\beta}^r uv}{u+v} - \grave{\alpha}^{1-r}\acute{\alpha}^r v, \end{cases} \tag{2.3}$$

where $0 \leq r \leq 1$.

2.2. Positivity and uniqueness

In this section, we prove the positivity and uniqueness of the solution of the fractional order model without a diffusion term.

The non-diffusion version of model (2.3) is as follows:

$$\begin{cases} D_t^{\alpha} u = u(1-u) - \frac{\grave{a}^{1-r}\acute{a}^r uv}{u+v} - \grave{b}^{1-r}\acute{b}^r u, \\ D_t^{\alpha} v = \frac{\acute{\beta}^{1-r}\grave{\beta}^r uv}{u+v} - \grave{\alpha}^{1-r}\acute{\alpha}^r v. \end{cases} \tag{2.4}$$

Theorem 2.3. *All solutions of the model system* (2.4) *are nonnegative.*

Proof. For a similar proof of Theorem (2.3), readers are referred to [19]. □

Theorem 2.4. *The fractional system* (2.4) *has a unique solution under any nonnegative initial conditions.*

Proof. According to the method proposed in [39–41], we define the following operator:

$$\begin{cases} f_1(t,u) = u(1-u) - \frac{\grave{a}^{1-r}\acute{a}^r uv}{u+v} - \grave{b}^{1-r}\acute{b}^r u, \\ f_2(t,v) = \frac{\acute{\beta}^{1-r}\grave{\beta}^r uv}{u+v} - \grave{\alpha}^{1-r}\acute{\alpha}^r v. \end{cases} \tag{2.5}$$

Let

$$N_1 = \underset{C_{a,b_1}}{sup}\|f_1(t,u)\|, N_2 = \underset{C_{a,b_2}}{sup}\|f_2(t,v)\|, \tag{2.6}$$

with

$$C_{a,b_1} = [t-a, t+a] \times [u-b_1, u+b_1] = A_1 \times B_1, \tag{2.7}$$

$$C_{a,b_2} = [t-a, t+a] \times [v-b_2, v+b_2] = A_2 \times B_2. \tag{2.8}$$

Using the Banach fixed point theorem, we can obtain the uniform norm:

$$\|f(t)\|_{\infty} = sup|f(t)|,\ t \in [t-a, t+a]. \tag{2.9}$$

The Picardis operator is as follows:

$$O : C(A_1, B_1, B_2) \to C(A_1, B_1, B_2). \tag{2.10}$$

This is defined as:

$$OX(t) = X_0(t) + \frac{1}{\Gamma(\alpha)} \int_0^t (t-\tau)^{\alpha-1} F(\tau, X(\tau))\, d\tau, \tag{2.11}$$

where $X(t) = [u(t), v(t)]^T$, $X_0(t) = [u_0(t), v_0(t)]^T$, and $F(t, X(t)) = [f_1(t,u), f_2(t,v)]^T$.

We assume that the solution of the model is bounded in a time period:

$$\|X(t)\|_{\infty} \leq \max\{b_1, b_2\}. \tag{2.12}$$

We can get:

$$\|OX(t) - X_0(t)\| = \|\frac{1}{\Gamma(\alpha)} \int_0^t (t-\tau)^{\alpha-1} F(\tau, X(\tau))\, d\tau\| \tag{2.13}$$

$$\leq \frac{1}{\Gamma(\alpha)} \int_0^t (t-\tau)^{\alpha-1} \|F(\tau, X(\tau))\| d\tau \leq \frac{Na^\alpha}{\Gamma(\alpha)} \leq aN \leq b, \tag{2.14}$$

with $N = \max\{N_1, N_2\}, b = \max\{b_1, b_2\}$, and $a < \frac{b}{N}$.

$$\|OX_1(t) - OX_2(t)\| = \|\frac{1}{\Gamma(\alpha)} \int_0^t (t-\tau)^{\alpha-1} \{F(\tau, X_1(\tau)) - F(\tau, X_2(\tau))\} d\tau\| \tag{2.15}$$

$$\leq \frac{1}{\Gamma(\alpha)} \int_0^t (t-\tau)^{\alpha-1} \|F(\tau, X_1(\tau)) - F(\tau, X_2(\tau))\| d\tau \tag{2.16}$$

$$\leq \frac{\beta}{\Gamma(\alpha)} \int_0^t (t-\tau)^{\alpha-1} \|X_1(\tau) - X_2(\tau)\| d\tau \tag{2.17}$$

$$\leq \frac{\beta a^\alpha}{\Gamma(\alpha)} \|X_1(\tau) - X_2(\tau)\| \leq a\beta \|X_1(\tau) - X_2(\tau)\|. \tag{2.18}$$

Since F is a contraction and $\beta < 1$, we obtain $a\beta < 1$, that is, the defined operator O is also a contraction. Therefore, the uniqueness proof of the system solution is complete. □

3. Stability and Hopf bifurcation analysis

Here, we determine the equilibrium point of the system (2.4). By analyzing the stability of the equilibrium point and the Hopf bifurcation, the conditions under which different states of the system appear are given.

3.1. Stability analysis

Before determining the stability of the equilibrium point, we first give the stability criterion of the fractional differential system.

Theorem 3.1. *([42, 43]) Consider a fractional differential system*

$$D_t^\alpha x(t) = f(t, x(t)). \tag{3.1}$$

Let x_* be an equilibrium point and the $\lambda_i, (i = 1, 2, \cdots, n)$ are eigenvalues of Jacobian matrix $J = \frac{\partial f}{\partial x_*}$.

1) The equilibrium point x_* is asymptotically stable if and only if

$$|arg(\lambda_i)| > \alpha\frac{\pi}{2}, i = 1, 2, \cdots, n. \tag{3.2}$$

2) The equilibrium point x_* is stable if and only if

$$|arg(\lambda_i)| \geq \alpha\frac{\pi}{2}, i = 1, 2, \cdots, n. \tag{3.3}$$

3) The equilibrium point x_* is unstable if and only if

$$\exists : |arg(\lambda_i)| < \alpha\frac{\pi}{2}, i = 1, 2, \cdots, n. \tag{3.4}$$

Definition 3.2. *([44]) The roots of the equation $f(t, x(t)) = 0$ are called the equilibria of fractional differential system*

$$D_t^{\alpha} x(t) = f(t, x(t)), \tag{3.5}$$

where $x(t) = (x_1(t), x_2(t), \cdots, x_n(t))^T \in \mathbb{R}^n$, $f(t, x(t)) \in R^n$, and $D_t^{\alpha} x(t) = (D_t^{\alpha_1} x_1(t), D_t^{\alpha_2} x_2(t), \cdots, D_t^{\alpha_n} x_n(t))^T$, $\alpha_i \in \mathbb{R}^+, i = 1, 2, \cdots, n$.

From a biological perspective, we are only interested in the positive equilibrium point. Obtain the equilibrium point by solving the following system of equations.

$$\begin{cases} f(u, v) = u(1-u) - \frac{\grave{a}^{1-r}\acute{a}^r uv}{u+v} - \grave{b}^{1-r}\acute{b}^r u, \\ g(u, v) = \frac{\acute{\beta}^{1-r}\grave{\beta}^r uv}{u+v} - \grave{\alpha}^{1-r}\acute{\alpha}^r v. \end{cases} \tag{3.6}$$

Denote by $f(u, v) = 0$ and $g(u, v) = 0$. The positive equilibrium point $E_* = (u_*, v_*)$ is obtained, where

$$u_* = \frac{\grave{a}^{1-r}\acute{a}^r\left(\acute{\alpha}^r\acute{\beta}^r\grave{\beta}^{-r}\grave{\alpha}^{1-r} - \acute{\beta}\right) - \grave{b}^{1-r}\acute{b}^r\acute{\beta} + \acute{\beta}}{\acute{\beta}}, \tag{3.7}$$

and

$$v_* = -\acute{\beta}^{1-r}\grave{\beta}^r\acute{\alpha}^{-r}\grave{\alpha}^{r-1}\left(\grave{a}^{1-r}\acute{a}^r + \grave{b}^{1-r}\acute{b}^r - 1\right) + \left(-\acute{a}^r\acute{\alpha}^r\grave{\beta}^{-r}\grave{\alpha}^{1-r}\acute{\beta}^{r-1} + 2\acute{a}^r\right)\grave{a}^{1-r} + \acute{b}^r\grave{b}^{1-r} - 1. \tag{3.8}$$

We can obtain the Jacobi matrix for system (3.6) at the equilibrium point E_* as follows:

$$J = \begin{pmatrix} a_{11} & a_{12} \\ a_{21} & a_{22} \end{pmatrix} = \begin{pmatrix} \frac{-\acute{a}^r\grave{a}^{1-r}v_*^2 - (u_*+v_*)^2\left(\acute{b}^r\grave{b}^{1-r} + 2u_* - 1\right)}{(u_*+v_*)^2} & \frac{-\acute{a}^r\grave{a}^{1-r}u_*^2}{(u_*+v_*)^2} \\ \frac{\acute{\beta}^{1-r}\grave{\beta}^r v_*^2}{(u_*+v_*)^2} & \frac{-\acute{\alpha}^r\grave{\alpha}^{1-r}(u_*+v_*)^2 + \acute{\beta}^{1-r}\grave{\beta}^r u_*^2}{(u_*+v_*)^2} \end{pmatrix}. \tag{3.9}$$

As such, the characteristic equation at equilibrium point E_* is read as follows:

$$\lambda^2 - tr_0\lambda + det_0 = 0, \tag{3.10}$$

where

$$tr_0 = a_{11} + a_{22}, \quad det_0 = a_{11}a_{22} - a_{21}a_{12}. \tag{3.11}$$

Roots of the characteristic equations are

$$\lambda_{1,2} = \frac{tr_0 \pm \sqrt{tr_0^2 - 4\det_0}}{2}. \tag{3.12}$$

Through Theorem (3.1), we draw the following conclusions:

Theorem 3.3. *([45]) The stability of equilibrium point E_* is determined by tr_0, det_0, and α.*

If $tr_0^2 - 4\det_0 \geq 0$, then,

1) The equilibrium point E_* is asymptotically stable if and only if $tr_0 \leq 0$ and $det_0 > 0$;
2) The equilibrium point E_* is unstable if and only if $tr_0 > 0$ or $det_0 < 0$.

If $tr_0^2 - 4\det_0 < 0$, then,

1) The equilibrium point E_* is stable if and only if $\alpha\frac{\pi}{2} < \left|\tan^{-1}\left(\frac{\sqrt{4\det_0 - tr_0^2}}{tr_0}\right)\right|$;
2) The equilibrium point E_* is unstable if and only if $\alpha\frac{\pi}{2} > \left|\tan^{-1}\left(\frac{\sqrt{4\det_0 - tr_0^2}}{tr_0}\right)\right|$.

Proof. The eigenvalues are real when $tr_0^2 - 4\det_0 \geq 0$.

For $tr_0 = 0$, $\lambda_{1,2} = \pm i\sqrt{\det_0}$ is obtained, therefore $\left|arg(\lambda_{1,2})\right| = \frac{\pi}{2} > \alpha\frac{\pi}{2}$ implies E_* is asymptotically stable; the eigenvalues are negative real when $tr_0 < 0$ and $det_0 > 0$, so $\left|arg(\lambda_{1,2})\right| = \pi > \alpha\frac{\pi}{2}$ implies E_* is asymptotically stable.

For $tr_0 > 0$ and $det_0 > 0$, both the eigenvalues are positive real, hence $\left|arg(\lambda_{1,2})\right| = 0 < \alpha\frac{\pi}{2}$ implies E_* is unstable; when $det_0 < 0$, the two eigenvalues are real numbers with opposite signs, so there exists $|arg(\lambda_1)| = 0 < \alpha\frac{\pi}{2}$ which implies that E_* is unstable.

The two eigenvalues are now complex conjugate when $tr_0^2 - 4\det_0 < 0$.

$$|arg(\lambda)| = \left|\tan^{-1}\left(\frac{\sqrt{4\det_0 - tr_0^2}}{tr_0}\right)\right|. \tag{3.13}$$

Therefore, E_* is stable if $\alpha\frac{\pi}{2} < \left|\tan^{-1}\left(\frac{\sqrt{4\det_0 - tr_0^2}}{tr_0}\right)\right|$ and is unstable for $\alpha\frac{\pi}{2} > \left|\tan^{-1}\left(\frac{\sqrt{4\det_0 - tr_0^2}}{tr_0}\right)\right|$. □

3.2. Hopf bifurcation analysis

When $tr_0 = 0$ and $det_0 > 0$, the system (2.4) with $\alpha = 1$ loses stability through Hopf bifurcation. Since the stability of system (2.4) is affected by the fractional derivative, the fractional derivative can be regarded as a parameter of Hopf bifurcation. In the following, we establish the conditions for the Hopf bifurcation of system (3.1) around E_* at parameter $\alpha = \alpha_h$ [19, 46]:

1) The Jacobian matrix at the equilibrium point E_* has a pair of complex conjugate eigenvalues $\lambda_{1,2} = a_i + ib_i$ which become purely imaginary at $\alpha = \alpha_h$;
2) $m(\alpha_h) = 0$ where $m(\alpha) = \alpha\frac{\pi}{2} - \min_{1\leq i\leq 2}|arg(\lambda_i)|$;
3) $\frac{\partial m(\alpha)}{\partial \alpha}\Big|_{\alpha=\alpha_h} \neq 0$.

Now, we prove that E_* has Hopf bifurcation when α goes through α_h.

Theorem 3.4. *Suppose that the equilibrium point E_* is unstable when $tr_0^2 - 4\det_0 < 0$ and $tr_0 > 0$. The fractional parameter α passes through the critical value α_h , and the system* (2.4) *undergoes Hopf bifurcation near E_*, where*

$$\alpha_h = \frac{2}{\pi}\tan^{-1}\left(\frac{\sqrt{4\det_0 - tr_0^2}}{tr_0}\right). \tag{3.14}$$

Proof. For $tr_0^2 - 4\det_0 < 0$ and $tr_0 > 0$, the eigenvalues are complex conjugates with a positive real part. Hence,

$$0 < arg(\lambda_{12}) = \tan^{-1}\left(\frac{\sqrt{4\det_0 - tr_0^2}}{tr_0}\right) < \frac{\pi}{2}, \tag{3.15}$$

and $\alpha\frac{\pi}{2} > \left|\tan^{-1}\left(\frac{\sqrt{4\det_0 - tr_0^2}}{tr_0}\right)\right|$ for some α. Let $\alpha_h\frac{\pi}{2} = \left|\tan^{-1}\left(\frac{\sqrt{4\det_0 - tr_0^2}}{tr_0}\right)\right|$, get $\alpha_h = \frac{2}{\pi}\tan^{-1}\left(\frac{\sqrt{4\det_0 - tr_0^2}}{tr_0}\right)$. Moreover, $\frac{\partial m(\alpha)}{\partial\alpha}\Big|_{\alpha=\alpha_h} = \frac{\pi}{2} \neq 0$. Therefore, all Hopf conditions satisfy. □

4. Turing instability

In this section, we present the Turing instability condition of the system (2.3) at $\alpha = 1$.

Perturbate the equilibrium point with $u = u_* + \tilde{u}, v = v_* + \tilde{v}$, substitute it into system (2.3), expand it through the Taylor series, and remove higher-order terms to obtain the linear perturbation equation

$$\dot{U} = JU + D\Delta U, \tag{4.1}$$

where

$$U = \begin{pmatrix} \tilde{u} \\ \tilde{v} \end{pmatrix}, D = \begin{pmatrix} d_1 & \\ & d_2 \end{pmatrix}, \tag{4.2}$$

and J is a Jacobian matrix about E_*. For convenience, we still denote $\tilde{u}$ and $\tilde{v}$ as u and v.

Expanding the perturbation variables in Fourier space and substituting $U = \begin{pmatrix} c_k^1 \\ c_k^2 \end{pmatrix} e^{\lambda t + ikr}$ into the perturbation Eq (4.1) yields the characteristic equation

$$\lambda\begin{pmatrix} c_k^1 \\ c_k^2 \end{pmatrix} = \begin{pmatrix} a_{11} - k^2 d_1 & a_{12} \\ a_{21} & a_{22} - k^2 d_2 \end{pmatrix}\begin{pmatrix} c_k^1 \\ c_k^2 \end{pmatrix}, \tag{4.3}$$

where λ is the growth rate, k is the wave number, r is the spatial vector, and c_k^1, c_k^2 are constants.

Solve characteristic Eq (4.3), and obtain the following dispersion relationship:

$$\lambda^2 - tr_k\lambda + det_k = 0, \tag{4.4}$$

where

$$\begin{cases} tr_k = a_{11} + a_{22} - k^2(d_1 + d_2) = tr_0 - k^2(d_1 + d_2), \\ \det_k = a_{11}a_{22} - a_{21}a_{12} - k^2(a_{11}d_2 + a_{22}d_1) + k^4 d_1 d_2 = \det_0 - k^2(a_{11}d_2 + a_{22}d_1) + k^4 d_1 d_2. \end{cases} \tag{4.5}$$

The solution of characteristic Eq (4.4) is in the following form:

$$\lambda_k = \frac{tr_k \pm \sqrt{tr_k^2 - 4\det_k}}{2}. \tag{4.6}$$

In order to explore the existence conditions of Turing instability at $k \neq 0$, we should ensure that $tr_k < 0$ and $det_k < 0$. When $\acute{a}^r \grave{a}^{1-r} > \acute{\beta}^{1-r} \grave{\beta}^r$, $tr_k < 0$ is easy to satisfy. In order to ensure the occurrence of $det_k < 0$, the condition of marginal stability $\min\left(\det_{k_c^2}\right) = 0$ should be satisfied. Here $k_c^2 = \frac{a_{11}d_2 + a_{22}d_1}{2d_1d_2}$ is the minimum value of det_k with respect to k_c^2.

From $\min\left(\det_{k_c^2}\right) = 0$, we can obtain:

$$a_{22}^2 d_1^2 + 2d_2 \left(a_{11}a_{22} - 2det_0\right) d_1 + a_{11}^2 d_2^2 = 0. \tag{4.7}$$

Let $H(d_1) = a_{22}^2 d_1^2 + 2d_2 \left(a_{11}a_{22} - 2det_0\right) d_1 + a_{11}^2 d_2^2$. If there are $H(d_1) = 0$ and $H(d_1) = -\min\left(\det_{k_c^2}\right)$, then there must be two roots, d_1^+ and d_1^-, where

$$d_1^+ = \frac{d_2\left(2\det_0 - a_{11}a_{22}\right) + 2d_2\sqrt{\det_0\left(\det_0 - a_{11}a_{22}\right)}}{a_{22}^2} > 0, \tag{4.8}$$

$$d_1^- = \frac{d_2\left(2\det_0 - a_{11}a_{22}\right) - 2d_2\sqrt{\det_0\left(\det_0 - a_{11}a_{22}\right)}}{a_{22}^2} > 0. \tag{4.9}$$

Theorem 4.1. *Suppose* $0 \leq r \leq 1, d_1 > 0, d_2 > 0$*, and* $\acute{a}^r \grave{a}^{1-r} > \acute{\beta}^{1-r} \grave{\beta}^r$ *are valid.*

1) The equilibrium point E_* is asymptotically stable if and only if $d_+^- < d_1 < d_1^+$;
2) The equilibrium point E_* is unstable if and only if $d_1 > d_+^-$ or $d_1 < d_+^-$;
3) Turing bifurcation occurs at $d_1 = d_+^-$ or $d_1 = d_+^-$, and the critical wave number is $k_c^2 = \sqrt{\frac{\det_0}{d_1^+ d_2}}$ or $k_c^2 = \sqrt{\frac{\det_0}{d_1^- d_2}}$.

Proof. The eigenvalues are negative real when $d_+^- < d_1 < d_1^+$, so $|arg(\lambda_k)| = \pi > \alpha\frac{\pi}{2}$ implies E_* is asymptotically stable. When $d_1 > d_+^-$ or $d_1 < d_+^-$, the two eigenvalues are real numbers with opposite signs, so there exists $|arg(\lambda_k)| = 0 < \alpha\frac{\pi}{2}$ which implies that E_* is unstable. From $\min\left(\det\left(k_c^2\right)\right) = 0$, we have $k_c^2 = \sqrt{\frac{\det_0}{d_1^+ d_2}}$ or $k_c^2 = \sqrt{\frac{\det_0}{d_1^- d_2}}$. □

Remark 4.2. *Take* $[\acute{a}, \grave{a}] = [1.31, 3.3]$, $[\acute{b}, \grave{b}] = [0.01, 0.04]$, $[\acute{\alpha}, \grave{\alpha}] = [0.5, 1.5]$, $[\acute{\beta}, \grave{\beta}] = [1.05, 1.5]$, $r = 1$, *and* $d_2 = 1.24$. *We have drawn the stable region of equilibrium point* E_* *on the plane when* $d_1 > 0, d_2 > 0$. *According to Theorem 4.1, the stable region and the unstable region are distinguished. The critical value* $d_1 = 0.1458$ *was obtained through fixed parameters in Figure 1(a). Furthermore, we draw a graph k about the wave number and the real part* λ *of the eigenvalue as shown in Figure 1(b).*

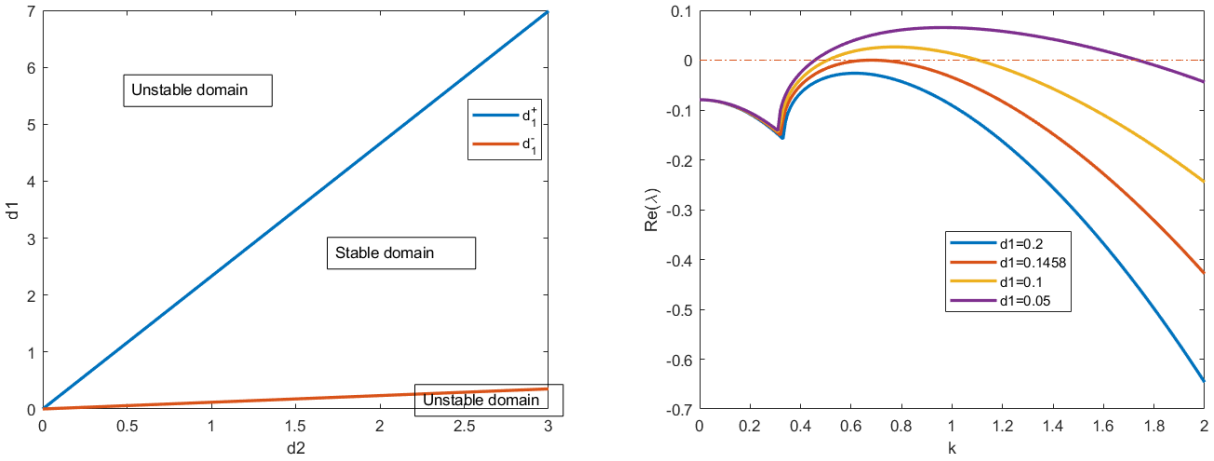

(a) Stability domains of the equilibrium E_*.

(b) The wave number of k corresponding to Re (λ) under different d_1.

Figure 1. Stability domains and wave number.

5. Weakly nonlinear analysis

In this section, we will use weak nonlinear analysis to calculate the amplitude equation near the Turing instability threshold $d_1 = d_1^c$. Write system (2.3) in the following form:

$$\frac{\partial U}{\partial t} = LU + N(U, U), \tag{5.1}$$

where L is a linear operator and N is a nonlinear operator

$$L = \begin{pmatrix} a_{11} + d_1\Delta & a_{12} \\ a_{21} & a_{22} + d_2\Delta \end{pmatrix}, \tag{5.2}$$

and

$$N = \begin{pmatrix} \frac{1}{2}f_{uu}u^2 + f_{uv}uv + \frac{1}{2}f_{vv}v^2 + \frac{1}{3!}f_{uuu}u^3 \\ +\frac{1}{2}f_{uuv}u^2v + \frac{1}{2}f_{uvv}uv^2 + \frac{1}{3!}f_{vvv}v^3 \\ \frac{1}{2}g_{uu}u^2 + g_{uv}uv + \frac{1}{2}g_{vv}v^2 + \frac{1}{3!}g_{uuu}u^3 \\ +\frac{1}{2}g_{uuv}u^2v + \frac{1}{2}g_{uvv}uv^2 + \frac{1}{3!}g_{vvv}v^3 \end{pmatrix} + O(4), \tag{5.3}$$

with

$$f_{uu} = \frac{2\acute{a}^r\grave{a}^{1-r}v_*^2 - 2(u_* + v_*)^3}{(u_* + v_*)^3}, f_{uv} = \frac{-2\acute{a}^r\grave{a}^{1-r}u_*v_*}{(u_* + v_*)^3}, f_{vv} = \frac{2\acute{a}^r\grave{a}^{1-r}u_*^2}{(u_* + v_*)^3}, \tag{5.4}$$

$$f_{uuu} = \frac{-6\acute{a}^r\grave{a}^{1-r}v_*^2}{(u_* + v_*)^4}, f_{uuv} = \frac{2\acute{a}^r\grave{a}^{1-r}v_*(2u_* - v_*)}{(u_* + v_*)^4}, f_{uvv} = \frac{-2\acute{a}^r\grave{a}^{1-r}u_*(u_* - 2v_*)}{(u_* + v_*)^4}, f_{vvv} = \frac{-6\acute{a}^r\grave{a}^{1-r}u_*^2}{(u_* + v_*)^4}, \tag{5.5}$$

$$g_{uu} = \frac{-2\grave{\beta}^r\acute{\beta}^{1-r}v_*^2}{(u_* + v_*)^3}, g_{uv} = \frac{2\grave{\beta}^r\acute{\beta}^{1-r}u_*v_*}{(u_* + v_*)^3}, g_{vv} = \frac{-2\grave{\beta}^r\acute{\beta}^{1-r}u_*^2}{(u_* + v_*)^3}, \tag{5.6}$$

$$g_{uuu} = \frac{6\grave{\beta}^r\acute{\beta}^{1-r}v_*^2}{(u_*+v_*)^4}, g_{uuv} = \frac{-2\grave{\beta}^r\acute{\beta}^{1-r}v_*(2u_*-v_*)}{(u_*+v_*)^4}, g_{uvv} = \frac{2\grave{\beta}^r\acute{\beta}^{1-r}u_*(u_*-2v_*)}{(u_*+v_*)^4}, g_{vvv} = \frac{6\grave{\beta}^r\acute{\beta}^{1-r}u_*^2}{(u_*+v_*)^4}. \quad (5.7)$$

We only consider the behavior of the control parameter near the bifurcation point, so the control parameter d_1 can be expanded as follows:

$$d_1 - d_1^c = \varepsilon d_{11} + \varepsilon^2 d_{12} + \varepsilon^3 d_{13} + O(4), \quad (5.8)$$

where ε is a small parameter. At the same time, the variable U and the nonlinear term N are expanded according to this small parameter:

$$U = \begin{pmatrix} u \\ v \end{pmatrix} = \varepsilon \begin{pmatrix} u_1 \\ v_1 \end{pmatrix} + \varepsilon^2 \begin{pmatrix} u_2 \\ v_2 \end{pmatrix} + \varepsilon^3 \begin{pmatrix} u_3 \\ v_3 \end{pmatrix} + O(4), \quad (5.9)$$

$$N = \varepsilon^2 N_2 + \varepsilon^3 N_3 + O\left(\varepsilon^4\right), \quad (5.10)$$

with

$$N_2 = \begin{pmatrix} \frac{1}{2}f_{uu}u_1^2 + f_{uv}u_1v_1 + \frac{1}{2}f_{vv}v_1^2 \\ \frac{1}{2}g_{uu}u_1^2 + g_{uv}u_1v_1 + \frac{1}{2}g_{vv}v_1^2 \end{pmatrix}, \quad (5.11)$$

and

$$N_3 = \begin{pmatrix} f_{uu}u_1u_2 + f_{uv}(u_1v_2 + u_2v_1) + f_{vv}v_1v_2 \\ +\frac{f_{uuu}}{3!}u_1^3 + \frac{f_{uuv}}{2!}u_1^2v_1 + \frac{f_{uvv}}{2!}u_1v_1^2 + \frac{f_{vvv}}{3!}v_1^3 \\ g_{uu}u_1u_2 + g_{uv}(u_1v_2 + u_2v_1) + g_{vv}v_1v_2 \\ +\frac{g_{uuu}}{3!}u_1^3 + \frac{g_{uuv}}{2!}u_1^2v_1 + \frac{g_{uvv}}{2!}u_1v_1^2 + \frac{g_{vvv}}{3!}v_1^3 \end{pmatrix}. \quad (5.12)$$

The linear operator L can be decomposed into

$$L = L_c + (d_1 - d_1^c)M, \quad (5.13)$$

where

$$L_c = \begin{pmatrix} a_{11} + d_1^c\Delta & a_{12} \\ a_{21} & a_{22} + d_2\Delta \end{pmatrix}, M = \begin{pmatrix} \Delta & 0 \\ 0 & 0 \end{pmatrix}. \quad (5.14)$$

We set $T_0 = t, T_1 = \varepsilon t, T_2 = \varepsilon^2 t$, and $T_3 = \varepsilon^3 t$, then the partial derivative of time can be written as follows:

$$\frac{\partial}{\partial t} = \varepsilon\frac{\partial}{\partial T_1} + \varepsilon^2\frac{\partial}{\partial T_2} + \varepsilon^3\frac{\partial}{\partial T_3} + O(4). \quad (5.15)$$

Substitute formulas (5.8)–(5.15) into Eq (5.1), and the left side of the equation becomes:

$$\varepsilon\frac{\partial}{\partial t}\begin{pmatrix} u_1 \\ v_1 \end{pmatrix} + \varepsilon^2\frac{\partial}{\partial t}\begin{pmatrix} u_2 \\ v_2 \end{pmatrix} + \varepsilon^3\frac{\partial}{\partial t}\begin{pmatrix} u_3 \\ v_3 \end{pmatrix} = \quad (5.16)$$

$$\varepsilon\left[\varepsilon\frac{\partial}{\partial T_1}\begin{pmatrix} u_1 \\ v_1 \end{pmatrix}+\varepsilon^2\frac{\partial}{\partial T_2}\begin{pmatrix} u_1 \\ v_1 \end{pmatrix}+\varepsilon^3\frac{\partial}{\partial T_3}\begin{pmatrix} u_1 \\ v_1 \end{pmatrix}\right]+\varepsilon^2\left[\varepsilon\frac{\partial}{\partial T_1}\begin{pmatrix} u_2 \\ v_2 \end{pmatrix}+\varepsilon^2\frac{\partial}{\partial T_2}\begin{pmatrix} u_2 \\ v_2 \end{pmatrix}+\varepsilon^3\frac{\partial}{\partial T_3}\begin{pmatrix} u_2 \\ v_2 \end{pmatrix}\right]+..., \tag{5.17}$$

and the right side of the equation becomes:

$$\left[L_c+\left(\varepsilon d_{11}+\varepsilon^2 d_{12}+\varepsilon^3 d_{13}\right)M\right]\left[\varepsilon\begin{pmatrix} u_1 \\ v_1 \end{pmatrix}+\varepsilon^2\begin{pmatrix} u_2 \\ v_2 \end{pmatrix}+\varepsilon^3\begin{pmatrix} u_3 \\ v_3 \end{pmatrix}\right]+\varepsilon^2 N_2+\varepsilon^3 N_3. \tag{5.18}$$

Comparing the order of ε on both sides of the equation, the following three cases are obtained:

$$\varepsilon: L_c\begin{pmatrix} u_1 \\ v_1 \end{pmatrix}=0, \tag{5.19}$$

$$\varepsilon^2: L_c\begin{pmatrix} u_2 \\ v_2 \end{pmatrix}=\frac{\partial}{\partial T_1}\begin{pmatrix} u_1 \\ v_1 \end{pmatrix}-d_{11}M\begin{pmatrix} u_1 \\ v_1 \end{pmatrix}-N_2, \tag{5.20}$$

$$\varepsilon^3: L_c\begin{pmatrix} u_3 \\ v_3 \end{pmatrix}=\frac{\partial}{\partial T_1}\begin{pmatrix} u_2 \\ v_2 \end{pmatrix}+\frac{\partial}{\partial T_2}\begin{pmatrix} u_1 \\ v_1 \end{pmatrix}-d_{11}M\begin{pmatrix} u_2 \\ v_2 \end{pmatrix}-d_{12}M\begin{pmatrix} u_1 \\ v_1 \end{pmatrix}-N_3. \tag{5.21}$$

They are discussed separately below. For $O(\varepsilon)$:

$$L_c\begin{pmatrix} u_1 \\ v_1 \end{pmatrix}=0. \tag{5.22}$$

That is, $\begin{pmatrix} u_1 \\ v_1 \end{pmatrix}$ is a linear combination of eigenvectors corresponding to eigenvalues of 0. Therefore,

$$\begin{pmatrix} a_{11}+d_1^c k_c^2 & a_{12} \\ a_{21} & a_{22}+d_2 k_c^2 \end{pmatrix}\begin{pmatrix} u_1 \\ v_1 \end{pmatrix}=0, \tag{5.23}$$

and the general solution of Eq (5.19) can be written as:

$$\begin{pmatrix} u_1 \\ v_1 \end{pmatrix}=\begin{pmatrix} \phi \\ 1 \end{pmatrix}\left(\sum_{j=1}^{3}A_j e^{ik_j r}+\sum_{j=1}^{3}\bar{A}_j e^{-ik_j r}\right), \tag{5.24}$$

where $\phi=-\frac{a_{22}+d_2k_c^2}{a_{21}}$, $|k_j|=k_c$, $k_c^2=\sqrt{\frac{\det_0}{d_1 d_2}}$, and k_j is the amplitude about the mode of $e^{-ik_j r}$. For $O\left(\varepsilon^2\right)$:

$$\begin{pmatrix} P_u \\ P_v \end{pmatrix}=\frac{\partial}{\partial T_1}\begin{pmatrix} u_1 \\ v_1 \end{pmatrix}-d_{11}M\begin{pmatrix} u_1 \\ v_1 \end{pmatrix}-N_2. \tag{5.25}$$

According to the de Fredholm solvability condition, the vector function at the right end of Eq (5.25) must be orthogonal to the zero eigenvalue of L_c^+ for this equation to have a nontrivial solution.

$$L_c^+=\begin{pmatrix} a_{11}+d_1^c\Delta & a_{21} \\ a_{12} & a_{22}+d_2\Delta \end{pmatrix}. \tag{5.26}$$

The zero eigenvector as:

$$\begin{pmatrix} 1 \\ \varphi \end{pmatrix} e^{-ik_j r} + c.c., \ j = 1, 2, 3, \tag{5.27}$$

with $\varphi = -\frac{a_{12}}{a_{22}+d_2 k_c^2}$. According to the orthogonal condition of Eq (5.20), we have

$$(1, \varphi) \begin{pmatrix} P_u^j \\ P_v^j \end{pmatrix} = 0, \ j = 1, 2, 3, \tag{5.28}$$

where P_u^j and P_v^j are the coefficients corresponding to $e^{ik_j r}$ in P_u and P_v. The system of equations related to amplitude A_j obtained from Eq (5.28) is:

$$\begin{cases} (\phi + \varphi) \frac{\partial A_1}{\partial T_1} = -d_{11} k_c^2 \phi A_1 + 2 (h_1 + \varphi h_2) \bar{A}_2 \bar{A}_3, \\ (\phi + \varphi) \frac{\partial A_2}{\partial T_1} = -d_{11} k_c^2 \phi A_2 + 2 (h_1 + \varphi h_2) \bar{A}_1 \bar{A}_3, \\ (\phi + \varphi) \frac{\partial A_3}{\partial T_1} = -d_{11} k_c^2 \phi A_3 + 2 (h_1 + \varphi h_2) \bar{A}_1 \bar{A}_2, \end{cases} \tag{5.29}$$

where $h_1 = \frac{f_{uu}}{2}\phi^2 + f_{uv}\phi + \frac{f_{vv}}{2}$, and $h_2 = \frac{g_{uu}}{2}\phi^2 + g_{uv}\phi + \frac{g_{vv}}{2}$. Introducing a second-order disturbance term as:

$$\begin{aligned} \begin{pmatrix} u_2 \\ v_2 \end{pmatrix} = \begin{pmatrix} U_0 \\ V_0 \end{pmatrix} + \sum_{j=1}^{3} \begin{pmatrix} U_j \\ V_j \end{pmatrix} e^{ik_j r} + \sum_{j=1}^{3} \begin{pmatrix} U_{jj} \\ V_{jj} \end{pmatrix} e^{2ik_j r} + \begin{pmatrix} U_{12} \\ V_{12} \end{pmatrix} e^{i(k_1 - k_2) r} + \\ \begin{pmatrix} U_{23} \\ V_{23} \end{pmatrix} e^{i(k_2 - k_3) r} + \begin{pmatrix} U_{31} \\ V_{31} \end{pmatrix} e^{i(k_3 - k_1) r} + c.c., \end{aligned} \tag{5.30}$$

Substitute formulas (5.24) and (5.30) into Eq (5.20), and we have

$$U_j = \phi V_j, \ j = 1, 2, 3, \qquad \begin{pmatrix} U_0 \\ V_0 \end{pmatrix} = \begin{pmatrix} u_0^0 \\ v_0^0 \end{pmatrix} \left(|A_1|^2 + |A_2|^2 + |A_3|^2 \right), \tag{5.31}$$

$$\begin{pmatrix} U_{jj} \\ V_{jj} \end{pmatrix} = \begin{pmatrix} u_1^1 \\ v_1^1 \end{pmatrix} A_j^2, \ j = 1, 2, 3, \qquad \begin{pmatrix} U_{ij} \\ V_{ij} \end{pmatrix} = \begin{pmatrix} u_2^2 \\ v_2^2 \end{pmatrix} A_i \bar{A}_j, \ i \neq j, i = j = 1, 2, 3, \tag{5.32}$$

with

$$\begin{aligned} \begin{pmatrix} u_0^0 \\ v_0^0 \end{pmatrix} &= \begin{pmatrix} \frac{2(a_{12}h_2 - a_{22}h_1)}{a_{11}a_{22} - a_{12}a_{21}} \\ \frac{2(a_{21}h_1 - a_{11}h_2)}{a_{11}a_{22} - a_{12}a_{21}} \end{pmatrix}, \\ \begin{pmatrix} u_1^1 \\ v_1^1 \end{pmatrix} &= \begin{pmatrix} \frac{a_{12}h_2 - \left(a_{22} - 4d_2 k_c^2\right) h_1}{\left(a_{11} - 4d_1^c k_c^2\right)\left(a_{22} - 4d_2 k_c^2\right) - a_{12}a_{21}} \\ \frac{a_{21}h_1 - \left(a_{11} - 4d_1 k_c^2\right) h_2}{\left(a_{11} - 4d_1^c k_c^2\right)\left(a_{22} - 4d_2 k_c^2\right) - a_{12}a_{21}} \end{pmatrix}, \\ \begin{pmatrix} u_2^2 \\ v_2^2 \end{pmatrix} &= \begin{pmatrix} \frac{2\left[a_{12}h_2 - \left(a_{22} - 3d_2 k_c^2\right) h_1\right]}{\left(a_{11} - 3d_1^c k_c^2\right)\left(a_{22} - 3d_2 k_c^2\right) - a_{12}a_{21}} \\ \frac{2\left[a_{21}h_1 - \left(a_{11} - 3d_1 k_c^2\right) h_2\right]}{\left(a_{11} - 3d_1^c k_c^2\right)\left(a_{22} - 3d_2 k_c^2\right) - a_{12}a_{21}} \end{pmatrix}. \end{aligned} \tag{5.33}$$

For $O\left(\varepsilon^3\right)$:

$$\begin{pmatrix} P_u \\ P_v \end{pmatrix} = \frac{\partial}{\partial T_1} \begin{pmatrix} u_2 \\ v_2 \end{pmatrix} + \frac{\partial}{\partial T_2} \begin{pmatrix} u_1 \\ v_1 \end{pmatrix} - d_{11} M \begin{pmatrix} u_2 \\ v_2 \end{pmatrix} - d_{12} M \begin{pmatrix} u_1 \\ v_1 \end{pmatrix} - N_3. \tag{5.34}$$

According to the orthogonal condition of Eq (5.21), we have

$$(1,\varphi)\begin{pmatrix} P_u^j \\ P_v^j \end{pmatrix} = 0,\ \ j = 1,2,3. \tag{5.35}$$

Direct calculation produces the amplitude equation:

$$\begin{cases} (\phi+\varphi)\left(\frac{\partial V_1}{\partial T_1}+\frac{\partial A_1}{\partial T_2}\right) = -k_c^2\phi\left(d_{11}V_1+d_{12}A_1\right)+2\left(h_1+\varphi h_2\right)\left(\bar{A}_2\bar{V}_3+\bar{A}_3\bar{V}_2\right) \\ \qquad\qquad +\left[\left(H_1+\varphi H_3\right)|A_1|^2+\left(H_2+\varphi H_4\right)\left(|A_2|^2+|A_3|^2\right)\right]A_1, \\ (\phi+\varphi)\left(\frac{\partial V_2}{\partial T_1}+\frac{\partial A_2}{\partial T_2}\right) = -k_c^2\phi\left(d_{11}V_2+d_{12}A_2\right)+2\left(h_1+\varphi h_2\right)\left(\bar{A}_1\bar{V}_3+\bar{A}_3\bar{V}_1\right) \\ \qquad\qquad +\left[\left(H_1+\varphi H_3\right)|A_2|^2+\left(H_2+\varphi H_4\right)\left(|A_1|^2+|A_3|^2\right)\right]A_2, \\ (\phi+\varphi)\left(\frac{\partial V_3}{\partial T_1}+\frac{\partial A_2}{\partial T_2}\right) = -k_c^2\phi\left(d_{11}V_3+d_{12}A_3\right)+2\left(h_1+\varphi h_2\right)\left(\bar{A}_2\bar{V}_1+\bar{A}_1\bar{V}_2\right) \\ \qquad\qquad +\left[\left(H_1+\varphi H_3\right)|A_3|^2+\left(H_2+\varphi H_4\right)\left(|A_2|^2+|A_1|^2\right)\right]A_3, \end{cases} \tag{5.36}$$

where

$$\begin{aligned} H_1 &= \left(\phi f_{uu}+f_{uv}\right)\left(u_0^0+u_1^1\right)+\left(\phi f_{uv}+f_{vv}\right)\left(v_0^0+v_1^1\right)+\tfrac{3\phi^3 f_{uuu}}{3!}+\tfrac{3\phi^2 f_{uuv}}{2!}+\tfrac{3\phi f_{uvv}}{2!}+\tfrac{3f_{vvv}}{3!}, \\ H_2 &= \left(\phi f_{uu}+f_{uv}\right)\left(u_0^0+u_2^2\right)+\left(\phi f_{uv}+f_{vv}\right)\left(v_0^0+v_2^2\right)+\tfrac{6\phi^3 f_{uuu}}{3!}+\tfrac{6\phi^2 f_{uuv}}{2!}+\tfrac{6\phi f_{uvv}}{2!}+\tfrac{6f_{vvv}}{3!}, \\ H_3 &= \left(\phi g_{uu}+g_{uv}\right)\left(u_0^0+u_1^1\right)+\left(\phi g_{uv}+g_{vv}\right)\left(v_0^0+v_1^1\right)+\tfrac{3\phi^3 g_{uuu}}{3!}+\tfrac{3\phi^2 g_{uuv}}{2!}+\tfrac{3\phi g_{uvv}}{2!}+\tfrac{3g_{vvv}}{3!}, \\ H_4 &= \left(\phi g_{uu}+g_{uv}\right)\left(u_0^0+u_2^2\right)+\left(\phi g_{uv}+g_{vv}\right)\left(v_0^0+v_2^2\right)+\tfrac{6\phi^3 g_{uuu}}{3!}+\tfrac{6\phi^2 g_{uuv}}{2!}+\tfrac{6\phi g_{uvv}}{2!}+\tfrac{6g_{vvv}}{3!}. \end{aligned} \tag{5.37}$$

Suppose that the perturbation of amplitude G under ε is as follows:

$$G = \varepsilon A_j + \varepsilon^2 V_j + O(3). \tag{5.38}$$

Then, from formulas (5.15), (5.29), (5.36), and (5.38), we can derive

$$\begin{cases} \tau_0\frac{\partial G_1}{\partial t} = \mu G_1 + h\bar{G}_2\bar{G}_3 - \left[g_1|G_1|^2+g_2\left(|G_2|^2+|G_3|^2\right)\right]G_1, \\ \tau_0\frac{\partial G_2}{\partial t} = \mu G_2 + h\bar{G}_1\bar{G}_3 - \left[g_1|G_2|^2+g_2\left(|G_1|^2+|G_3|^2\right)\right]G_2, \\ \tau_0\frac{\partial G_3}{\partial t} = \mu G_3 + h\bar{G}_1\bar{G}_2 - \left[g_1|G_3|^2+g_2\left(|G_1|^2+|G_2|^2\right)\right]G_3, \end{cases} \tag{5.39}$$

with

$$\mu = \frac{d_{1\text{-}}d_1^c}{d_1^c}, \tau_0 = \frac{\phi+\varphi}{d_1^c k_c^2}, h = \frac{2\left(h_1+\varphi h_2\right)}{d_1^c k_c^2}, g_1 = -\frac{H_1+\varphi H_3}{d_1^c k_c^2},\ \textit{and}\ g_2 = -\frac{H_2+\varphi H_4}{d_1^c k_c^2}. \tag{5.40}$$

Since each amplitude $A_j = \rho_j e^{i\psi_j}\,(j=1,2,3)$ in Eq (5.39) can be decomposed into mode $\rho_j = |A_j|$ and phase angle ψ_j, substituting A_j into Eq (5.39) to separate the real and imaginary parts yields the following equation:

$$\begin{cases} \frac{\partial\psi}{\partial t} = -h\frac{\rho_1^2\rho_2^2+\rho_1^2\rho_3^2+\rho_2^2\rho_3^2}{\rho_1\rho_2\rho_3}\sin\psi, \\ \frac{\partial\rho_1}{\partial t} = \mu\rho_1+h\rho_2\rho_3\cos\psi-g_1\rho_1^3-g_2\left(\rho_2^2+\rho_3^2\right)\rho_1, \\ \frac{\partial\rho_1}{\partial t} = \mu\rho_1+h\rho_2\rho_3\cos\psi-g_1\rho_1^3-g_2\left(\rho_2^2+\rho_3^2\right)\rho_1, \\ \frac{\partial\rho_1}{\partial t} = \mu\rho_1+h\rho_2\rho_3\cos\psi-g_1\rho_1^3-g_2\left(\rho_2^2+\rho_3^2\right)\rho_1, \end{cases} \tag{5.41}$$

where $\psi = \psi_1+\psi_2+\psi_3$. We can infer from Eq (5.41) that the solution to the equation is stable when $h>0, \psi=0$ and $h<0, \psi=\pi$. Eq (5.41) has the following solutions:

1) Stationary state:

$$\rho_1 = \rho_2 = \rho_3 = 0, \tag{5.42}$$

stable when $\mu < \mu_2 = 0$, and unstable when $\mu > \mu_2 = 0$.

2) Strip pattern:

$$\rho_1 = \sqrt{\frac{\mu}{g_1}} \neq 0, \rho_2 = \rho_3 = 0, \tag{5.43}$$

stable when $\mu > \mu_3 = \frac{h^2 g_1}{(g_2-g_1)^2}$, and unstable when $\mu < \mu_3 = \frac{h^2 g_1}{(g_2-g_1)^2}$.

3) Hexagon pattern:
When $\mu > \mu_1 = \frac{-h^2}{4(g_1+2g_2)}$ is satisfied, there exists

$$\rho_1 = \rho_2 = \rho_3 = \frac{|h| \pm \sqrt{h^2 + 4(g_1+2g_2)\mu}}{2(g_1+2g_2)}. \tag{5.44}$$

When $\mu < \mu_4 = \frac{(2g_1+g_2)h^2}{(g_2-g_1)^2}$, $\rho^+ = \frac{|h|+\sqrt{h^2+4(g_1+2g_2)\mu}}{2(g_1+2g_2)}$ is stable, and $\rho^- = \frac{|h|-\sqrt{h^2+4(g_1+2g_2)\mu}}{2(g_1+2g_2)}$ is always unstable.

4) Mixed state:
When $\mu > \mu_3 = \frac{h^2 g_1}{(g_2-g_1)^2}$ is satisfied, there exists

$$\rho_1 = \frac{|h|}{g_2 - g_1}, \rho_2 = \rho_3 = \sqrt{\frac{\mu - g_1\rho_1^2}{g_1 + g_2}}. \tag{5.45}$$

It is always unstable with $g_1 < g_2$.

6. Numerical simulation

In this section, we use the Euler discrete method for numerical simulation in two-dimensional space $\Omega = [0, L_x] \times \left[0, L_y\right]$. Choose $L_x = 200, L_y = 200, t = 1000$, time step $\Delta t = 0.9$, and space step $\Delta h = 2$. We define $u_{pq}^n = u\left(x_p, y_q, n\Delta t\right)$ and $v_{pq}^n = v\left(x_p, y_q, n\Delta t\right)$ where $p, q = 1, 2, \cdots, \frac{L_x}{\Delta h}$. System (2.3) is discretized by the Euler method as follows:

$$\begin{cases} \frac{u_{pq}^{n+1}-u_{pq}^n}{\Delta t} = d_1 \Delta u_{pq}^n + u_{pq}^n\left(1 - u_{pq}^n\right) - \frac{\grave{a}^{1-r}\acute{a}^r u_{pq}^n v_{pq}^n}{u_{pq}^n + v_{pq}^n} - \grave{b}^{1-r}\acute{b}^r u_{pq}^n, \\ \frac{v_{pq}^{n+1}-v_{pq}^n}{\Delta t} = d_2 \Delta v_{pq}^n + \frac{\acute{\beta}^{1-r}\grave{\beta}^r u_{pq}^n v_{pq}^n}{u_{pq}^n + v_{pq}^n} - \grave{\alpha}^{1-r}\acute{\alpha}^r v_{pq}^n, \end{cases}$$

where

$$\Delta u_{pq} = \frac{u_{p+1,q} + u_{p-1,q} + u_{p,q+1} + u_{p,q-1} - 4u_{pq}}{h^2},$$
$$\Delta v_{pq} = \frac{v_{p+1,q} + v_{p-1,q} + v_{p,q+1} + v_{p,q-1} - 4v_{pq}}{h^2}.$$

The parameters in system (2.3) are selected as follows:

$$[\acute{a}, \grave{a}] = [1.31, 3.3], [\acute{b}, \grave{b}] = [0.01, 0.04], [\acute{\alpha}, \grave{\alpha}] = [0.5, 1.5], [\acute{\beta}, \grave{\beta}] = [1.05, 1.5],$$

$$r = 1, d_1 = 0.1, d_2 = 1.24, d_1^c = 0.1458,$$

and then, we obtain

$$E_* = (0.11667, 0.23333), \mu = -0.31413, \mu_1 = 0.13029, \mu_2 = 0, \mu_3 = -2.59739, \mu_4 = -6.23184,$$
$$g_1 = -294.62990, \text{ and } g_2 = -117.63726.$$

The initial data are as follows:

$$u(x, y, 0) = u_* (1 + 0.1 (rand - 0.5)), v(x, y, 0) = v_* (1 + 0.1 (rand - 0.5)).$$

The numerical simulation results show that there is a mixed structure solution under this set of parameters, and there are spots and stripe patterns in the graphics, as shown in Figure 2.

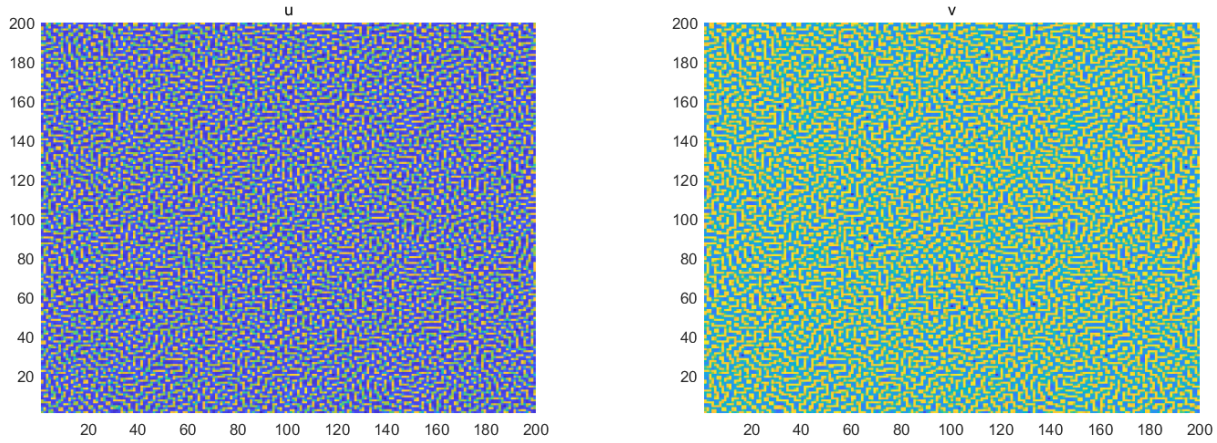

(a) $r = 1$. (b) $r = 1$.

Figure 2. Asymmetric mixed pattern solutions of u and v. Here $[\acute{a}, \grave{a}] = [1.31, 3.3]$, $[\acute{b}, \grave{b}] = [0.01, 0.04]$, $[\acute{\alpha}, \grave{\alpha}] = [0.5, 1.5]$, $[\acute{\beta}, \grave{\beta}] = [1.05, 1.5]$, $d_1 = 0.1, d_2 = 1.24$, and $d_1^c = 0.1458$.

Under the same parameters, changing $r = 0.6$ yields $E_* = (0.21788, 0.14732)$, $\mu = -0.31413$, $\mu_3 = -4.52393$, $g_1 = -15680.19532$, and $g_2 = -20512.90109$. The numerical results show that there are also mixed structure solutions under this set of parameters, as seen in Figure 3.

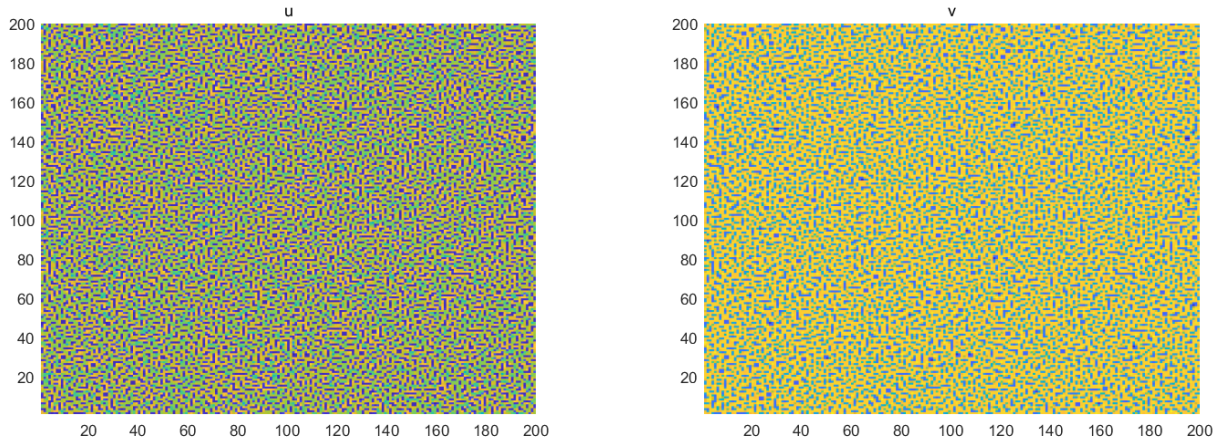

(a) $r = 0.6$ (b) $r = 0.6$

Figure 3. Asymmetric mixed pattern solutions of u and v. Here $[\acute{a},\ \grave{a}] = [1.31, 3.3]$, $[\acute{b}, \grave{b}] = [0.01, 0.04]$, $[\acute{\alpha}, \grave{\alpha}] = [0.5, 1.5]$, $[\acute{\beta}, \grave{\beta}] = [1.05, 1.5]$, $d_1 = 0.1$, $d_2 = 1.24$, and $d_1^c = 0.1458$.

Although we only change the interval variable r in the graph, it can still be seen that the interval variable r will affect the positive equilibrium point E_* and the critical value d_1^c of the Turing instability. Therefore, these two spatial patterns are slightly different and also prove the correctness of the theory.

Select the following symmetric initial conditions:

$$u(x, y, 0) = \begin{cases} u_* + 0.5, & x, y \in (80, 120), \\ u_* - 0.001, & other. \end{cases}$$

$$v(x, y, 0) = \begin{cases} v_* + 0.25, & x, y \in (80, 120), \\ v_* - 0.001, & other. \end{cases}$$

Applying symmetric initial conditions, numerical simulations are performed with varying the parameters r, t, and d_1 while other parameters remain constant, and the results show the existence of a symmetric hybrid structure solution, as seen in Figure 4. The figure shows the detailed pattern evolution of symmetric mixed patterns under different parameters. At first, circular patterns begin to appear under the initial conditions. As time t progresses, the bounded domain is gradually destroyed and the circular pattern decomposes into striped and spotted patterns. It is found that as the diffusion rate d_1 of the prey population increases, the spatiotemporal chaos of the model is gradually suppressed.

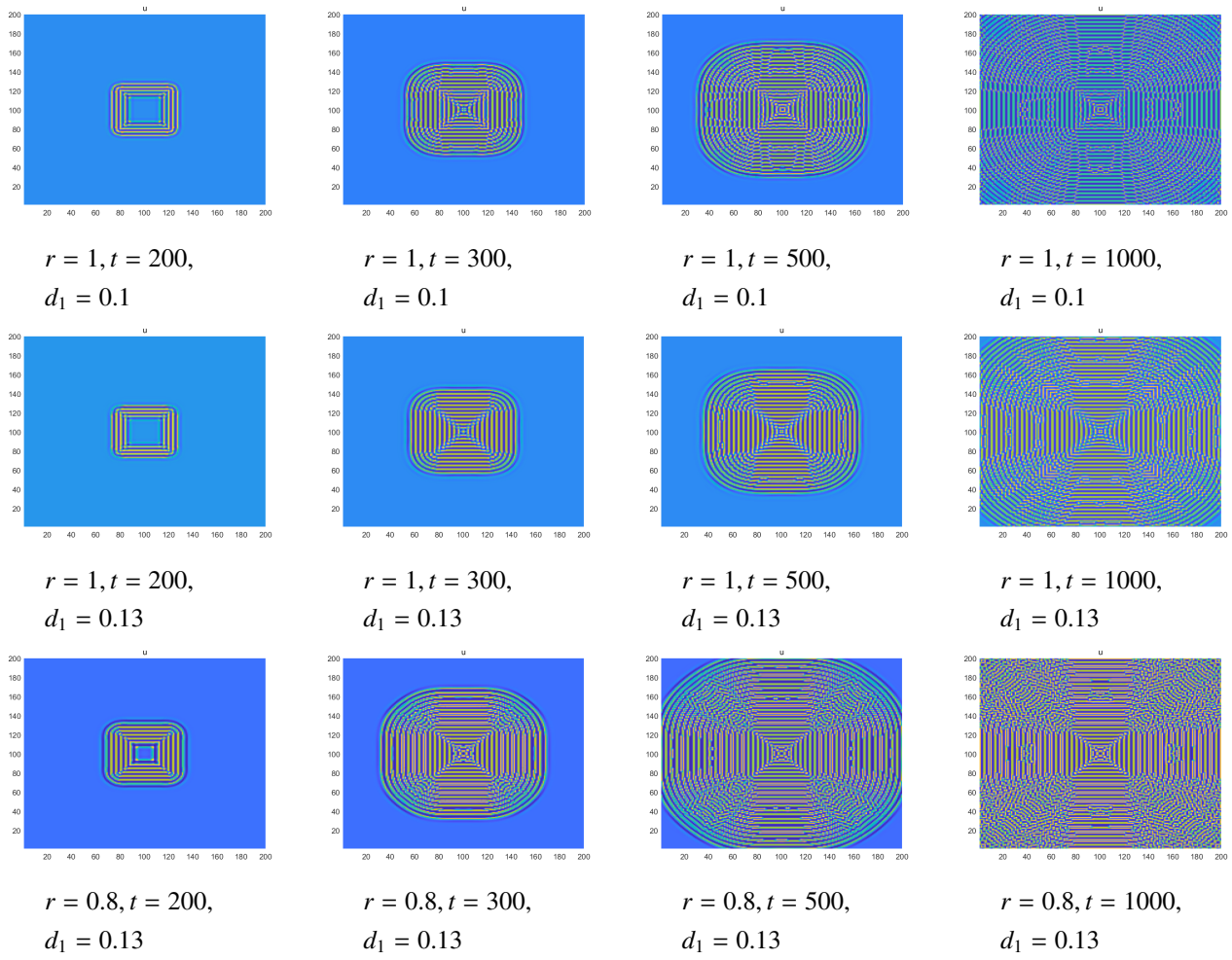

$r = 1, t = 200,$ $d_1 = 0.1$ | $r = 1, t = 300,$ $d_1 = 0.1$ | $r = 1, t = 500,$ $d_1 = 0.1$ | $r = 1, t = 1000,$ $d_1 = 0.1$

$r = 1, t = 200,$ $d_1 = 0.13$ | $r = 1, t = 300,$ $d_1 = 0.13$ | $r = 1, t = 500,$ $d_1 = 0.13$ | $r = 1, t = 1000,$ $d_1 = 0.13$

$r = 0.8, t = 200,$ $d_1 = 0.13$ | $r = 0.8, t = 300,$ $d_1 = 0.13$ | $r = 0.8, t = 500,$ $d_1 = 0.13$ | $r = 0.8, t = 1000,$ $d_1 = 0.13$

Figure 4. The evolution of u under different parameters. Here $[\acute{a}, \grave{a}] = [1.31, 3.3]$, $[\acute{b}, \grave{b}] = [0.01, 0.04]$, $[\acute{\alpha}, \grave{\alpha}] = [0.5, 1.5]$, $[\acute{\beta}, \grave{\beta}] = [1.05, 1.5]$, $d_2 = 1.24$, and $d_1^c = 0.1458$.

7. Conclusions

In this paper, the predator-prey model with an interval biological coefficient was analyzed theoretically and simulated numerically. We proved the existence and uniqueness of the model solution, discussed the stability of the positive equilibrium point, studied the Hopf bifurcation around the equilibrium point related to the fractional parameter α, and discussed the Turing instability of the model at the starting point $d_1 = d_1^-$. It was found that the fractional α and the diffusion term d_1 played an important role in controlling the existence of the Hopf bifurcation and Turing instability. Then, the amplitude equation near the threshold of the Turing instability was given by using the weak nonlinear analysis method, and different mode selections were classified by using the amplitude equation. Finally, through numerical simulation, we showed the symmetric and asymmetric patterns of the model, and found that the diffusion rate of the prey population inhibited the spatiotemporal chaos of the model.

Author contributions

Conceptualization: Xiao-Long Gao and Hao-Lu Zhang; Methodology and software: Xiao-Yu Li; Data curation, formal analysis, and funding acquisition: Xiao-Long Gao and Xiao-Yu Li; Writing-original draft and writing-review and editing: Xiao-Long Gao, Hao-Lu Zhang, and Xiao-Yu Li. All authors have read and agreed to the published version of the manuscript.

Use of AI tools declaration

The authors declare they have not used Artificial Intelligence (AI) tools in the creation of this article.

Acknowledgements

This paper is supported by the doctoral research start-up Fund of Inner Mongolia University of Technology (DC2300001252).

Conflicts of interest

The authors declare that there are no conflicts of interest regarding the publication of this article.

References

1. Z. M. Bi, S. T. Liu, M. Ouyang, Spatial dynamics of a fractional predator-prey system with time delay and Allee effect, *Chaos Soliton. Fract.*, **162** (2022), 112434. https://doi.org/10.1016/j.chaos.2022.112434
2. M. X. Chen, R. C. Wu, Steady states and spatiotemporal evolution of a diffusive predator-prey model, *Chaos Soliton. Fract.*, **170** (2023), 113397. https://doi.org/10.1016/j.chaos.2023.113397
3. M. Y. Qian, Y. T. Huang, Y. R. Cao, J. Y. Wu, Y. M. Xiong, Ecological network construction and optimization in Guangzhou from the perspective of biodiversity conservation, *J. Environ. Manage.*, **336** (2023), 117692. https://doi.org/10.1016/j.jenvman.2023.117692
4. J. Bhattacharyya, A. Chatterjee, Dynamics of a fishery model with contions therhold harvesting policy and its leverage for conservation and management, *J. Biol. Syst.*, **30** (2022), 913–943. https://doi.org/10.1142/S0218339022500334
5. X. P. Yan, C. H. Zhang, Global stability of a delayed diffusive predator-prey model with prey harvesting of Michaelis-Menten type, *Appl. Math. Lett.*, **114** (2021), 106904. https://doi.org/10.1016/j.aml.2020.106904
6. W. Ou, C. J. Xu, Q. Y. Cui, Y. C. Pang, Z. X. Liu, J. W. Shen, et al., Hopf bifurcation exploration and control technique in a predator-prey system incorporating delay, *AIMS Mathematics*, **9** (2024), 1622–1651. https://doi.org/10.3934/math.2024080
7. Y. Yao, Bifurcations of a Leslie Gower predator-prey system with ratiodependent Holling IV functional response and prey harvesting, *Math. Method. Appl. Sci.*, **43** (2020), 2137–2170. https://doi.org/10.1002/mma.5944

8. F. R. Zhang, X. H. Zhang, Y. Li, C. P. Li, Hopf bifurcation of a delayed predator-prey model with nonconstant death rate and constant-rate prey harvesting, *Int. J. Bifurcat. Chaos*, **28** (2018), 1850179. https://doi.org/10.1142/S0218127418501791

9. M. X. Chen, S. Ham, Y. Choi, H. Kim, J. Kim, Pattern dynamics of a harvested predator-prey model, *Chaos Soliton. Fract.*, **176** (2023), 114153. https://doi.org/10.1016/j.chaos.2023.114153

10. Q. Y. Cui, C. J. Xu, W. Ou, Y. C. Pang, Z. X. Liu, P. L. Li, et al., Bifurcation behavior and hybrid controller design of a 2D Lotka-Volterra commensal symbiosis system accompanying delay, *Mathematics*, **11** (2023), 4808. https://doi.org/10.3390/math11234808

11. Q. L. Wang, Z. J. Liu, X. G. Zhang, R. A. Cheke, Incorporating prey refuge into a predator-prey system with imprecise parameter estimates, *Comp. Appl. Math.*, **36** (2017), 1067–1084. https://doi.org/10.1007/s40314-015-0282-8

12. D. Pal, G. S. Mahapatra, G. P. Samanta, A study of bifurcation of prey-predator model with time delay and harvesting using fuzzy parameters, *J. Biol. Syst.*, **26** (2018), 339–372. https://doi.org/10.1142/S021833901850016X

13. X. Y. Meng, Y. Q. Wu, Dynamical analysis of a fuzzy phytoplankton-zooplankton model with refuge, fishery protection and harvesting, *J. Appl. Math. Comput.*, **63** (2020), 361–389. https://doi.org/10.1007/s12190-020-01321-y

14. M. Liu, M. Fan, Permanence of stochastic Lotka-Volterra systems, *J. Nonlinear Sci.*, **27** (2017), 425–452. https://doi.org/10.1007/s00332-016-9337-2

15. A. Hening, D. H. Nguyen, Stochastic Lotka-Volterra food chains, *J. Math. Biol.*, **77** (2018), 135–163. https://doi.org/10.1007/s00285-017-1192-8

16. D. Pal, G. S. Mahaptra, G. P. Samanta, Optimal harvesting of prey-predator system with interval biological parameters: A bioeconomic model, *Math. Biosci.*, **241** (2013), 181–187. https://doi.org/10.1016/j.mbs.2012.11.007

17. M. Ramezanadeh, M. Heidari, O. S. Fard, A. H. Borzabadi, On the interval differential equation: novel solution methodology, *Adv. Differ. Equ.*, **2015** (2015), 338. https://doi.org/10.1186/s13662-015-0671-8

18. U. Ghosh, B. Mondal, M. S. Rahman, S. Sarkar, Stability analysis of a three species food chain model with linear functional response via imprecise and parametric approach, *J. Comput. Sci.-Neth.*, **54** (2021), 101423. https://doi.org/10.1016/j.jocs.2021.101423

19. E. Balci, Predation fear and its carry-over effect in a fractional order prey-predator model with prey refuge, *Chaos Soliton. Fract.*, **175** (2023), 114016. https://doi.org/10.1016/j.chaos.2023.114016

20. C. Han, Y. L. Wang, Z. Y. Li, A high-precision numerical approach to solving space fractional Gray-Scott model, *Appl. Math. Lett.*, **125** (2022), 107759. https://doi.org/10.1016/j.aml.2021.107759

21. C. Han, Y. L. Wang, Z. Y. Li, Novel patterns in a class of fractional reaction-diffusion models with the Riesz fractional derivative, *Math. Comput. Simulat.*, **202** (2022), 149–163. https://doi.org/10.1016/j.matcom.2022.05.037

22. J. Ning, Y. L. Wang, Fourier spectral method for solving fractional-in-space variable coefficient KdV-Burgers equation, *Indian J. Phys.*, **98** (2024), 1727–1744. https://doi.org/10.1007/s12648-023-02934-2

23. Y. Galviz, G. M. Souza, U. Lüttge, The biological concept of stress revisited: relations of stress and memory of plants as a matter of space-time, *Theor. Exp. Plant Physiol.*, **34** (2022), 239–264. https://doi.org/10.1007/s40626-022-00245-1

24. C. J. Xu, M. X. Liao, P. L. Li, L. Y. Yao, Q. W. Qin, Y. L. Shang, Chaos control for a fractional-order Jerk system via time delay feedback controller and mixed controller, *Fractal Fract.*, **5** (2021), 257. https://doi.org/10.3390/fractalfract5040257

25. T. Patel, H. Patel, An analytical approach to solve the fractional-order (2 + 1)-dimensional Wu-Zhang equation, *Math. Method. Appl. Sci.*, **46** (2023), 479–489. https://doi.org/10.1002/mma.8522

26. T. Patel, R. Meher, Adomian decomposition sumudu transform method for solving a solid and porous fin with temperature dependent internal heat generation, *SpringerPlus*, **5** (2016), 489. https://doi.org/10.1186/s40064-016-2106-8

27. C. Han, Y. L. Wang, Z. Y. Li, Numerical solutions of space fractional variable-coefficient kdv-modified kdv equation by Fourier spectral method, *Fractals*, **29** (2021), 2150246. https://doi.org/10.1142/S0218348X21502467

28. X. Y. Li, C. Han, Y. L. Wang, Novel patterns in fractional-in-space nonlinear coupled fitzHugh-Nagumo models with Riesz fractional derivative, *Fractal Fract.*, **6** (2022), 136. https://doi.org/10.3390/fractalfract6030136

29. F. Z. Tian, Y. L. Wang, Z. Y. Li, Numerical simulation of soliton propagation behavior for the fractional-in-space NLSE with variable coefficients on unbounded domain, *Fractal Fract.*, **8** (2024), 163. https://doi.org/10.3390/fractalfract8030163

30. C. Han, Y. L. Wang, Numerical solutions of variable-coefficient fractional-in-space KdV equation with the Caputo fractional derivative, *Fractal Fract.*, **6** (2022), 207. https://doi.org/10.3390/fractalfract6040207

31. Y. L. Wang, L. N. Jia, H. L. Zhang, Numerical solution for a class of space-time fractional equation by the piecewise reproducing kernel method, *Int. J. Comput. Math.*, **96** (2019), 1544367. https://doi.org/10.1080/00207160.2018.1544367

32. M. X. Chen, Q. Q. Zheng, Diffusion-driven instability of a predator-prey model with interval biological coefficients, *Chaos Soliton. Fract.*, **172** (2023), 113494. https://doi.org/10.1016/j.chaos.2023.113494

33. X. L. Gao, H. L. Zhang, Y. L. Wang, Z. Y. Li, Research on pattern dynamics behavior of a fractional vegetation-water model in arid flat environment, *Fractal Fract.*, **8** (2024), 264. https://doi.org/10.3390/fractalfract8050264

34. W. F. Tang, Y. L. Wang, Z. Y. Li, Numerical simulation of fractal wave propagation of a multi-dimensional nonlinear fractional-in-space Schrödinger equation, *Phys. Scr.*, **98** (2023), 045205. https://doi.org/10.1088/1402-4896/acbdd0

35. X. L. Gao, Y. L. Wang, Z. Y. Li, Chaotic dynamic behavior of a fractional-order financial systems with constant inelastic demand, in press.

36. Z. Y. Li, Q. T. Chen, Y. L. Wang, X. Y. Li, Solving two-sided fractional super-diffusive partial differential equations with variable coefficients in a class of new reproducing kernel spaces, *Fractal Fract.*, **6** (2022), 492. https://doi.org/10.3390/fractalfract6090492

37. A. Khan, H. Khan, J. F. Gómez-Aguilar, T. Abdeljawad, Existence and Hyers-Ulam stability for a nonlinear singular fractional differential equations with Mittag-Leffler kernel, *Chaos Soliton. Fract.*, **127** (2019), 422–427. https://doi.org/10.1016/j.chaos.2019.07.026

38. A. Devi, A. Kumar, T. Abdeljawad, A. Khan, Stability analysis of solutions and existence theory of fractional Lagevin equation, *Alex. Eng. J.*, **60** (2021), 3641–3647. https://doi.org/10.1016/j.aej.2021.02.011

39. A. Atangana, I. Koca, Chaos in a simple nonlinear system with Atangana-Baleanu derivatives with fractional order, *Chaos Soliton. Fract.*, **89** (2016), 447–454. https://doi.org/10.1016/j.chaos.2016.02.012

40. A. Devi, A. Kumar, D. Baleanu, A. Khan, On stability analysis and existence of positive solutions for a general non-linear fractional differential equations, *Adv. Differ. Equ.*, **2020** (2020), 300. https://doi.org/10.1186/s13662-020-02729-3

41. X. R. Lin, Y. C. Wang, J. F. Wang, W. X. Zeng, Dynamic analysis and adaptive modified projective synchronization for systems with Atangana-Baleanu-Caputo derivative: A financial model with nonconstant demand elasticity, *Chaos Soliton. Fract.*, **160** (2022), 112269. https://doi.org/10.1016/j.chaos.2022.112269

42. K. Baisad, S. Moonchai, Analysis of stability and Hopf bifurcation in a fractional Gauss-type predator-prey model with Allee effect and Holling type-III functional response, *Adv. Differ. Equ.*, **2018** (2018), 82. https://doi.org/10.1186/s13662-018-1535-9

43. I. Petráš, *Fractional-order nonlinear systems: modeling, analysis and simulation*, Heidelberg: Springer, 2011. https://doi.org/10.1007/978-3-642-18101-6

44. W. H. Deng, J. H. Lü, Generating multi-directional multi-scroll chaotic attractors via a fractional differential hysteresis system, *Phys. Lett. A*, **369** (2007), 438–443. https://doi.org/10.1016/j.physleta.2007.04.112

45. U. Ghosh, S. Pal, M. Banerjee, Memory effect on Bazykin's prey-predator model: Stability and bifurcation analysis, *Chaos Soliton. Fract.*, **143** (2021), 110531. https://doi.org/10.1016/j.chaos.2020.110531

46. D. Barman, J. Roy, H. Alrabaiah, P. Panja, S. P. Mondal, S. Alam, Impact of predator incited fear and prey refuge in a fractional order prey predator model, *Chaos Soliton. Fract.*, **142** (2021), 110420. https://doi.org/10.1016/j.chaos.2020.110420

AIMS Press